RESEARCH ARTICLE

Kaposi's Sarcoma-Associated Herpesvirus Genome Programming during the Early Stages of Primary Infection of Peripheral Blood Mononuclear Cells

Hem C. Jha,[a] Jie Lu,[a] Subhash C. Verma,[b] Shuvomoy Banerjee,[a] Devan Mehta,[a] Erle S. Robertson[a]

Department of Microbiology and Tumor Virology Program of the Abramson Cancer Center, Perelman School of Medicine at the University of Pennsylvania, Philadelphia, Pennsylvania, USA[a]; Department of Microbiology and Immunology, School of Medicine, University of Nevada, Reno, Nevada, USA[b]

H.C.J. and J.L. contributed equally to this article.

ABSTRACT **The early period of Kaposi's sarcoma-associated herpesvirus (KSHV) infection involves the dynamic expression of viral genes, which are temporally and epigenetically regulated. KSHV can effectively infect and persist in endothelial as well as human B cells with different gene expression patterns. To understand the temporal epigenetic changes which occur when KSHV infects the lymphocytic compartment, we infected human peripheral blood mononuclear cells (PBMCs) and comprehensively analyzed the changes which occurred at the binding sites of virally encoded lytic as well as latent proteins along with epigenetic modifications across the KSHV genome during early primary infection. Using chromatin immunoprecipitation (ChIP) assays, we showed that the KSHV genome acquires a uniquely distinct histone modification pattern of methylation (H3K4me3, H3K9me3, and H3K27me3) and acetylation (H3Ac) during *de novo* infection of human PBMCs. This pattern showed that the epigenetic changes were temporally controlled. The binding profiles of KSHV latent protein LANA and the immediate early proteins RTA and K8 showed specific patterns at different times postinfection, which reflects the gene expression program. Further analysis demonstrated that KSHV can concurrently express lytic and latent genes which were associated with histone modifications at these specific regions on the viral genome. We identified three KSHV genes, K3, ORF49, and ORF64, which exhibited different profiles of histone modifications during the early stages of PBMC infection. These studies established a distinct pattern of epigenetic modification which correlates with viral gene expression temporally regulated during the first 7 days of PBMC infection and provides clues to the regulatory program required for successful infection by KSHV of human PBMCs.**

IMPORTANCE **Kaposi's sarcoma-associated herpesvirus (KSHV) has been documented as one of the major contributors to morbidity and mortality in AIDS patients during the AIDS pandemic. During its life cycle, KSHV undergoes latent and lytic replication. Typically, KSHV maintains a stringent preference for latent infection in the infected B cells. However, 1 to 5% of infected cells undergo spontaneous lytic reactivation. KSHV lytic replication and infection of new cells are likely to be critical for maintaining the population of infected cells which drive virus-associated pathogenesis. Here, we explored the temporal changes of crucial histone marks on the KSHV genome during early infection of human primary peripheral blood mononuclear cells (PBMCs), which are a physiologically relevant system for monitoring primary infection. These results showed that KSHV possessed a distinct pattern of epigenetic marks during early infection of PBMCs. Further, KSHV concurrently expressed lytic and latent genes during this early period. These results now provide new evidence which contributes to understanding the molecular mechanism that regulates viral gene expression during early infection.**

Received 6 November 2014 **Accepted** 10 November 2014 **Published** 16 December 2014

Citation Jha HC, Lu J, Verma SC, Banerjee S, Mehta D, Robertson ES. 2014. Kaposi's sarcoma-associated herpesvirus genome programming during the early stages of primary infection of peripheral blood mononuclear cells. mBio 5(6):e02261-14. doi:10.1128/mBio.02261-14.

Editor Michael J. Imperiale, University of Michigan

Address correspondence to Erle S.Robertson, erle@mail.med.upenn.edu.

This article is a direct contribution from a Fellow of the American Academy of Microbiology.

Kaposi's sarcoma-associated herpesvirus (KSHV), a human gammaherpesvirus, is closely associated with development of at least two lymphoproliferative disorders, primary effusion lymphoma (PEL) and multicentric Castleman's disease (MCD), as well as a vascular cancer, Kaposi's sarcoma (KS) (1–4). KS is a tumor of lymphatic endothelial origin commonly seen in AIDS patients (5). PEL, also referred to as body cavity-based lymphoma (BCBL), is a non-Hodgkin's lymphoma characterized by liquid tumor growth in body cavities (6). PEL occurs predominantly but not exclusively in HIV-positive patients with advanced AIDS (7, 8). It is aggressive and progresses rapidly with a high mortality rate. The mean survival time for patients with PEL is approximately 2 to 6 months (9). KSHV is also associated with most cases of MCD arising in patients infected with HIV (10). KSHV-MCD, a rare B-cell lymphoproliferative disorder that affects lymph nodes and other lymphoid tissue, is a rapidly progressing aggres-

sive tumor, which can lead to death (10, 11). These lymphoproliferative diseases are closely associated with KSHV-infected B cells. However, the molecular mechanisms which trigger the development of KSHV-mediated lymphoproliferative diseases are not completely understood.

KSHV infections in endothelial cells are fairly well elucidated (12, 13). Recently, Chandran's group showed that KSHV infection induces reactive oxygen species (ROS) during early infection to promote its efficient entry via macropinocytosis in HMVEC-d cells (14). For KSHV infection of primary B cells, two groups have shown that KSHV infects a subset of tonsillar B cells driving plasmablast differentiation and proliferation and that KSHV-encoded viral FLICE-inhibitory protein (vFLIP) induces B-lymphocyte transdifferentiation and tumorigenesis in animal models (15, 16). T and B lymphocytes in primary human tonsils can be infected by KSHV, with B lymphocytes producing a substantial amount of infectious virus progeny (17, 18). During its life span, KSHV expresses latent and lytic cycle proteins. Our previous studies showed that RBP-Jκ regulates the promoters of LANA and RTA in a reciprocal manner (19–21). Recently, we generated a recombinant KSHV with a deletion of the RBP-Jκ site within the LANA promoter (LANAp) (22). This virus showed that the RBP-Jκ site was critical for the establishment of latent infection in primary cells, as mutation of this site resulted in increased lytic replication during infection of human peripheral blood mononuclear cells (PBMCs) (22). In contrast, recombinant KSHVs deleted for the RBP-Jκ binding sites within the RTA promoter showed enhanced viral latency with a substantial decrease in lytic replication during primary infection of human PBMCs (23). Here, we utilized those recombinant viruses to further explore the temporal and epigenetic changes of KSHV latent and lytic genomes during primary infection.

The impact of epigenetic changes on gene expression without altering the DNA sequence can have a global effect on the genome and occurs through DNA methylation and histone modifications (24, 25). DNA methylation occurs at CpG sites, which are repeats of a cytosine nucleotide followed by a guanine nucleotide (26). A CpG island adjacent to a transcription initiation site is generally associated with repression or silencing of transcription, and hypermethylation of CpG islands is a common epigenetic alteration associated with cancer (27). Histone modifications include acetylation, methylation, phosphorylation, ubiquitylation, and citrullination (28). Typically, epigenetic changes on DNA and histones are important contributors to tumor progression (29). Epigenetic modifications are frequently found in KSHV-associated cancer. Interestingly, KSHV microRNA (miRNA) targets the viral immediate early protein RTA and the cellular factor Rbl2 to regulate global epigenetic reprogramming (30). KSHV also regulates the host epigenetic modifier EZH2 to promote angiogenesis (31). Recently, epigenetic analysis of KSHV latent and lytic genomes (32) and epigenetic modifications of the KSHV genome by methylated DNA immunoprecipitation (MeDIP) assay in the long-term infected SLK cell line were examined (33). These studies showed profound epigenetic changes across the KSHV genome during lytic and latent infection (32). Furthermore, the KSHV RTA promoter exhibited a bivalent promoter structure to flexibly regulate both latent and lytic infections by KSHV (33). Here, we explored the epigenetic changes of the KSHV genome in a physiologically relevant background during early infection in human PBMCs, important for establishment of persistent infection in the lymphocytic compartment.

The KSHV genome possesses very low redundancy and is comprised of an approximately 140-kbp long unique coding region with 53.5% GC content, which encodes ~86 open reading frames (ORFs). Many regions of the genome are still not well characterized (34). The early steps of KSHV infection are a dynamic process and involve collaboration of viral genes that are temporally expressed due to various epigenetic modifications of their regulatory regions. In this study, we used human PBMCs to explore KSHV infection using a physiologically relevant primary cell background. Our previous data have shown that KSHV efficiently infects human PBMCs (22, 23). Here, we focused on the dynamic changes in KSHV gene expression and the epigenetic programming using activation markers H3K4me3 and H3Ac and repression markers H3K9me3 and H3K27me3 that occur during the first 7 days after infection of human PBMCs. These studies contribute to our understanding of the molecular mechanisms that regulate viral gene expression to successfully establish latent infection in human PBMCs. Collectively, this study elucidates a mechanism of KSHV genome programming during the early stages of KSHV infection.

RESULTS

The KSHV genome undergoes distinct epigenetic changes during primary infection. Early infection by gammaherpesviruses is a multistep complex process, which involves a series of temporal interactions between multiple viral antigens and host cell factors. KSHV infection requires a series of highly regulated steps, which include virus-receptor interactions, entry, intracellular trafficking, and a highly specialized viral and host gene expression program (13). Previously, we have demonstrated that KSHV can successfully infect human PBMCs for up to 7 days (22, 23). Here, we analyzed a genome-wide response during these early steps of PBMC infection. Human PBMCs (40×10^6) were infected with purified KSHV virions and incubated for 1, 2, 4, and 7 days. Chromatin immunoprecipitation (ChIP) assays for histone modifications were performed on those infected PBMCs using the antibodies against H3K4me3, H3K9me3, H3K27me3, and H3Ac (Fig. 1). ChIP DNAs were assayed by quantitative real-time PCR (qPCR) using the KSHV genome-wide primer sets amplifying 250- to 500-bp regions across the entire KSHV genome. An enrichment of targets greater than 2-fold over the respective isotype control antibody was considered significant.

Histone H3 exhibited active as well as repressive modifications through methylation across the KSHV genome during infection of human PBMCs. Significant modifications of trimethylated histone H3 lysine 4 (H3K4me3) and H3K27me3 were seen throughout the KSHV genome from 1 day to 7 days postinfection (p.i.) (Fig. 1). The viral genes associated with H3K4me3 modifications were localized at three major KSHV gene clusters (15 to 25 kb, 70 to 80 kb, and 105 to 120 kb). There, highly methylated DNAs were found in KSHV-positive latently infected BCBL1 cell lines but not in the *de novo*-infected endothelial SLK cell line (SLKp) (33). H3K4me3 modifications at the genomic regions 15 to 25 kb and 70 to 80 kb were seen in noninduced TRExBCBL1-RTA cells. However, the modification at genomic region 105 to 120 kb was not detected in these cells (32). In contrast to these earlier studies, the BCBL1 viral genome also had widely distributed H3K27me3

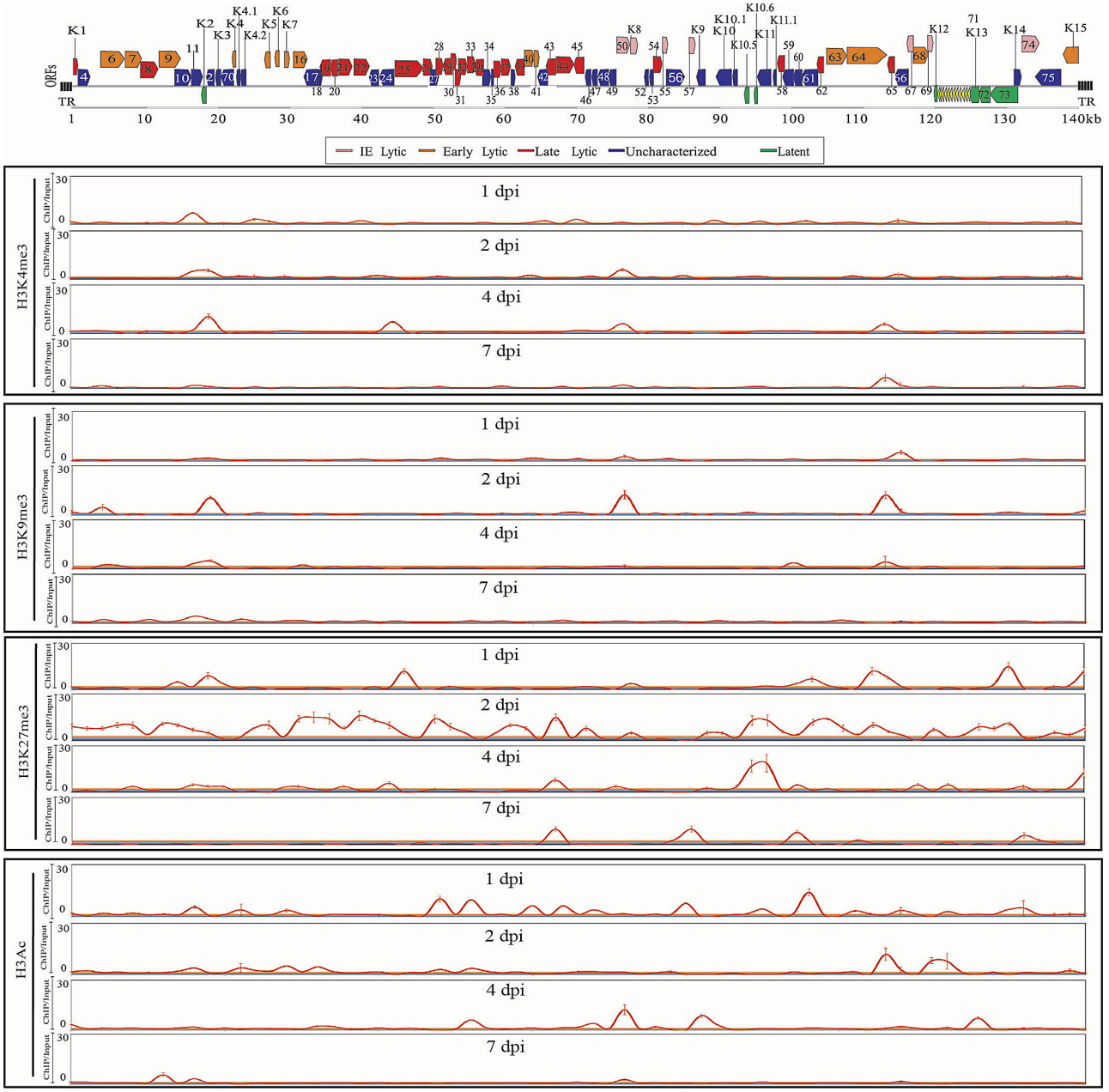

FIG 1 Global patterns of histone modification across KSHV genome during early primary infection. The histone modification ChIP assays were performed with wt KSHV-infected PBMCs at 1, 2, 4, and 7 days p.i. using the antibodies for histone H3K4me3, H3K9me3, H3K27me3, and H3Ac. ChIP DNA was assayed by quantitative PCR using a genome-wide array of primers across the KSHV genome. Approximate KSHV genome positions are indicated on the top of the panel. IE, immediate early; dpi, days postinfection.

marks, emphasizing trends similar to those in KSHV-infected PBMCs observed in this study (32).

The trimethylated histone H3 lysine 9 (H3K9me3) exhibited a distinct enrichment at KSHV genomic regions 5 to 10 kb, 15 to 25 kb, 70 to 80 kb, 105 to 120 kb, and 130 to 140 kb from 1 day to 7 days p.i. during primary PBMC infection (Fig. 1). This pattern peaked at these regions at 2 days p.i. but became more diffused by 7 days p.i. with a pattern that seems to be throughout the genome but at lower intensities (Fig. 1). Interestingly, these regions with methylation modifications were consistent with those reported in previous BCBL1 cells (33). However, no significant modification of H3K9me3 was found except for the genomic region 105 to 120 kb in the latent TRExBCBL1-RTA cell background (32). In addition, histone H3 acetylation (H3Ac) marks were enriched throughout the KSHV genome at 1 day p.i. but less so by 7 days p.i. (Fig. 1). The KSHV genomic region at 30 to 50 kb during primary PBMC infection was consistent with previous studies with a reduced or minimal change in H3Ac (32). However, the H3Ac marks were distributed at genomic regions 10 to 25 kb, 70 to 80 kb, and 130 to 140 kb but not enriched within the 105- to 120-kb

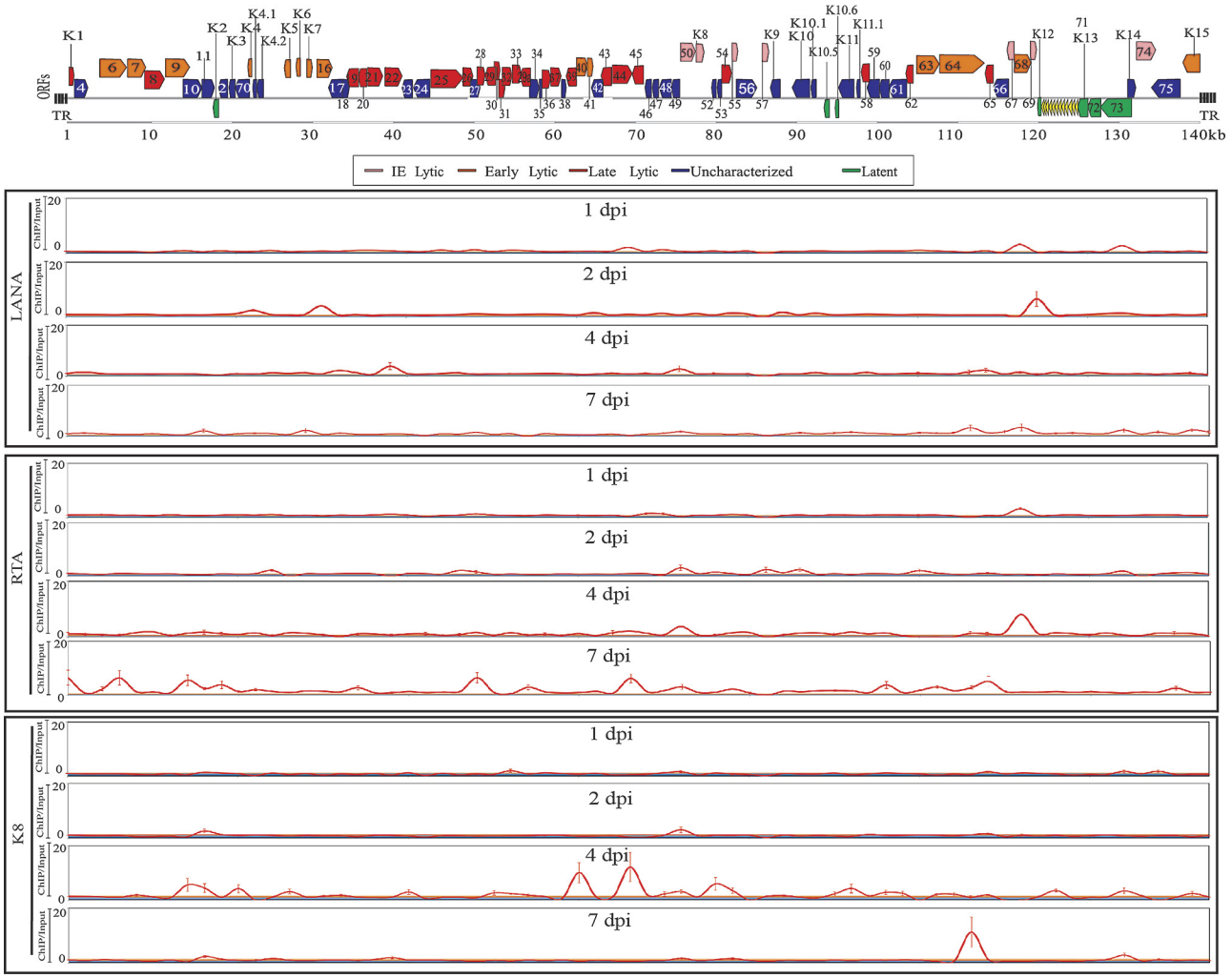

FIG 2 Analysis of KSHV latency and lytic life cycle during early primary infection at 1, 2, 4, and 7 days p.i. ChIP assays were performed with wt KSHV-infected human PBMCs using the antibody for KSHV latent protein LANA and lytic proteins RTA and K8. ChIP DNAs were assayed by quantitative PCR using a genome-wide array of primers across the KSHV genome. Approximate KSHV genome positions are written on the top of the panel. IE, immediate early; dpi, days postinfection.

region in BCBL1 cells and SLKp cells (35). These results are indicative of a different pattern of epigenetic modification across the KSHV genome during early primary PBMC infection from the patterns seen in BCBL1 and SLKp cells. This may reflect a pattern of epigenetic regulation of the KSHV genome which is unique for primary PBMC infection and could be important for latency establishment.

Distinct regions of the KSHV genome are regulated by LANA, RTA, and K8 during infection of human PBMCs. During infection of primary lymphocytes, KSHV strives to establish latent infection by expressing genes capable of modulating and reprograming the host signaling pathways. Both latent and lytic gene expression programs occur simultaneously during the early stages of primary infection (36). Therefore, we hypothesized that KSHV activates multiple genes involved in latent as well as lytic replication to successfully complete the early steps of infection, which ultimately leads to establishment of a latent infection. Here, we used antibodies against the KSHV latent protein LANA and the lytic proteins RTA and K8 to perform ChIP assays to identify the KSHV genomic regions associated with these virus-encoded latent and lytic regulatory proteins during early primary PBMC infection (Fig. 2). The results of genome-wide ChIP assay showed that the KSHV major latent protein LANA associated with viral DNA primarily at three genomic regions, 20 to 40 kb, 108 to 120 kb, and 130 to 140 kb, which included a number of lytic and latent genes (Fig. 2). Moreover, the association with LANA was more uniform at 7 days p.i. throughout the genome, compared to a more focused association at 2 and 4 days post-infection of PBMCs. Recent studies have also shown that the genomic regions 20 to 40 kb and 130 to 140 kb were regulated by LANA in the BCBL1 cells (37). However, the genomic region 130 to 140 kb did not show high enrichment with LANA in the BCBL1 cells (37). This indicates that this region may be important for establishment of KSHV latency after infection of PBMCs.

The major immediate early protein RTA showed association with a wide range of genomic regions across the entire genome, including regions 1 to 10 kb, 20 to 30 kb, 50 to 55 kb, 70 to 80 kb, and 110 to 120 kb (Fig. 2). Interestingly, the regions enriched by

RTA antibody were not consistent with the previous study in latently infected BCBL1 cells (38). This suggests that RTA regulates different regions of the KSHV genome during early PBMC infection. K8 was enriched at the genomic regions 20 to 30 kb, 60 to 80 kb, 105 to 115 kb, and 125 to 140 kb, suggesting that K8 is likely to be actively involved in activating the lytic gene expression program during KSHV early infection (Fig. 2). The data shown here suggest that KSHV can utilize its latent as well as lytic proteins to regulate its latent and lytic program genes transcribed during the first few days of PBMC infection.

Epigenetic modifications and gene regulation on the KSHV genome during PBMC infection. The results from the ChIP assays using various antibodies against histone modifications (H3K4me3, H3K9me3, H3K27me3, and H3Ac) showed that the KSHV genome is temporally modified with histone methylations and acetylation marks during primary infection of PBMCs. H3K4me3 occupancy on the KSHV genome was typically increased from 1 day to 4 days p.i., indicating occurrence of an active chromatin modification during early primary infection which is regulated in a time-dependent manner (Fig. 1). In contrast, H3K9me3 and H3K27me3 enrichment plateaued at 2 days p.i. and then declined after 4 days, suggesting that the repressive marks were generated first, which was followed by the active mark H3K4me3 on the viral genome during early infection (Fig. 1). Specifically, H3K9me3 and H3K27me3 established a stronger enrichment throughout the genome by 2 days p.i. than did H3K4me3, although similar peaks were seen at 2 days p.i. for both H3K4me3 and H3K9me3 (Fig. 1). These data strongly suggest that KSHV utilizes a mechanism which involves temporal regulation of epigenetic marks during PBMC infection. Furthermore, histone acetylation (H3Ac) was readily detected from 1 day to 4 days p.i., suggesting that H3Ac was also important during the early steps of KSHV infection in PBMCs. Remarkably, the repressive epigenetic modifications were generally suppressed at 7 days p.i. compared to the modifications at 1 day to 4 days p.i. of the repressive marks (Fig. 1). These results indicate that these changes in epigenetic modifications are important for KSHV primary infection and a successful establishment of latency.

The ChIP data showed that LANA, RTA, and K8 bound to a number of genomic regions to concurrently regulate virus-carried genes from both the latent and lytic programs during the early stages of primary infection (Fig. 2). An increase in association of LANA with viral DNA from 1 day to 4 days p.i. was seen, and the neighboring genes suggest that LANA may bind to regions that regulate these viral ORFs to stimulate their expression during the early stages of primary infection. In contrast, the major lytic proteins RTA and K8 associated with a wide range of viral genes and regulatory regions across the entire genome (Fig. 2). ChIP results with RTA showed an enhanced enrichment at regions which include ORFs across the viral genome that were temporally regulated as seen from 1 day to 7 days p.i. (Fig. 2). This suggested that RTA plays a major role in regulation of genes across the KSHV genome during the early stages of primary infection. Interestingly, RTA enrichment was more robust at 7 days p.i. across the KSHV genome and overlapped in some regions with LANA enrichment at the KSHV genome. In addition, immunoprecipitation of viral DNA bound to K8 also showed a significant enrichment across the KSHV genome from 1 day to 7 days p.i. (Fig. 2). However, the strongest association was seen at 4 days postinfection, and this tapered off at 7 days p.i. Notably, the enrichment of RTA on the KSHV genome was seen later than that for K8 (7 days p.i. compared to 4 days p.i.), indicating that K8 may be required much earlier as it relates to its contribution to viral lytic replication during the early period of PBMC infection. It is interesting that LANA as well as RTA and K8 was enriched at the regulatory regions of ORF50, suggesting involvement in its control (Fig. 2).

Epigenetic modifications on the KSHV genome are coordinated with viral gene expression during primary infection. Epigenetic programming of herpesviral genomes plays an important role in transcriptional regulation of latent and lytic genes during the viral life cycle (32). The data above showed that viral genes associated with histone H3 methylation and acetylation occurred at three major KSHV genome clusters (8 to 30 kb, 53 to 80 kb, and 105 to 130 kb). H3K4me3 modifications were associated with genomic regions which include genes involved in antiapoptosis (ORF16), DNA replication (ORF49, ORF56, ORF59, and ORF70), oncogenesis (K3), and virion particle assembly (ORF25, ORF29b, ORF45, ORF64, and ORF65) (Fig. 1 and Table 1). H3K27me3 modifications on the KSHV genome during primary infection were widespread and efficiently occurred at many regions on the viral genome, including genes related to functions associated with antiapoptosis, DNA replication, oncogenesis, immunomodulation, regulation of transmembrane protein, and virion particle assembly (Fig. 1 and Table 1). H3K9me3 modifications on the KSHV genome were linked to regulation of the transmembrane proteins (ORF4 and ORF7), virion structural proteins (ORF64 and ORF65), and proteins involved in the oncogenic process (K3 and K15) (Fig. 1 and Table 1). The H3Ac ChIP assay showed acetylation of a number of H3-associated regions across the KSHV genome, including regions encoding ORF11, K3, ORF18, ORF29a, ORF36, ORF42, ORF49, ORF59, ORF64, ORF68, and ORF69 (Fig. 1 and Table 1), which have a wide range of functions and are dispersed throughout the KSHV genome.

The results of genome-wide ChIP assays showed that the KSHV major latent protein LANA associated with the regulatory regions of a number of lytic and latent genes (Fig. 2 and Table 1). The LANA-ChIP assay showed that LANA associated with viral DNA which carries lytic and latent ORFs, including K3, K7, K15, ORF18, ORF19, ORF25, ORF49, ORF64, ORF65, ORF68, ORF69, and ORF73. This suggests that KSHV may establish latent infection in PBMCs by activating a specific program of gene expression, which includes both latent and lytic genes. Further, a look at KSHV genomic regions associated with the lytic protein RTA showed that it binds to a large number of ORFs spread across the KSHV genome (Fig. 2 and Table 1). The viral genes bound by RTA belonged to a group of transmembrane proteins (ORF4, ORF7, ORF22, ORF68), virion proteins (ORF29a, ORF32, ORF45, and ORF64), and capsid proteins (ORF62, ORF65, and ORF75) and also included genes involved in transcription regulation (ORF49 and ORF70) with some overlap for those also bound to LANA (Fig. 2 and Table 1). Therefore, as expected, RTA can regulate the expression of proteins involved in synthesis of virus particles and virion release. The viral genomic regions bound by K8 were mostly associated with DNA replication (ORF59), transcription regulation (K8 and ORF49), virion proteins (ORF17, ORF27, ORF42, and ORF45), and oncogenesis (ORF34, ORF73, K3, K11.1, and K12) (Fig. 2 and Table 1), suggesting that K8 is involved in promoting viral replication during early primary infection.

On closer examination, we found that three major domains/clusters of viral genes were temporally bound to LANA, RTA, and

TABLE 1 Summary of KSHV ORFs with epigenetic modifications (H3K4me3, H3K9me3, H3K27me3, and H3Ac) and associated with LANA, RTA, and K8 proteins during primary PBMC infection[b]

Classification	KSHV ORF	Name	Associated function	Enrichment[a]						
				LANA	RTA	K8	H3K4me3	H3K9me3	H3Ac	H3K27me3
	ORF02	DHFR	Dihydrofolate reductase		+	+				+
	ORF04		Complement binding protein		+			+	+	+
E	ORF06	SSB	Single-strand binding protein							+
E	ORF07		Transport protein		+			+		+
L	ORF08	gB	Glycoprotein							+
E	ORF09	POL	DNA polymerase							+
	ORF10		Derived from the herpesvirus dUTPase					+		
	ORF11		Derived from the herpesvirus dUTPase						+	+
E	ORF16	vBcl-2	Viral homolog of Bcl-2, antiapoptotic		+		+			+
E	ORF17		Viral protease/ capsid protein			+				+
	ORF18		*trans* factor, for late gene transcription	+					+	
E	ORF19		Tegument protein	+						+
L	ORF20		Inducers of cell cycle arrest							
E	ORF21	TK	Thymidine kinase						+	+
L	ORF22	gH	Glycoprotein		+					+
	ORF23		Tegument protein							
	ORF24		Related to HHV-5 UL87							+
L	ORF25		Major capsid protein	+			+			+
L	ORF26		Minor capsid antigen							
L	ORF27		Virion proteins (unclassified)			+	+			+
L	ORF28		Membrane protein							
E	ORF29a		Packaging protein		+				+	+
IE	ORF29b		Packaging protein							+
L	ORF30		Related to HHV-5 UL91							
E	ORF31		MHV ORF31, required for viral replication							+
L	ORF32		Tegument protein		+					
L	ORF33		Tegument							
	ORF34	HRE	Hypoxia, HRE			+				+
	ORF35		Associated *in vitro* infection							
E	ORF36		Phosphotransferase/ serine protein kinase						+	+
E	ORF37	SOX	Shutoff and exonuclease		+					

(Continued on following page)

TABLE 1 (Continued)

Classification	KSHV ORF	Name	Associated function	Enrichment[a]						
				LANA	RTA	K8	H3K4me3	H3K9me3	H3Ac	H3K27me3
	ORF38	g/M?	Myristylated tegument protein							
L	ORF39	gM	Glycoprotein							
E	ORF40	PAF	Primase-associated factor							+
E	ORF41	PAF	Primase-associated factor	+						
L	ORF42		Tegument protein			+	+		+	+
L	ORF43		Capsid protein							
E	ORF44	HEL	Helicase						+	+
IE	ORF45		Tegument, phosphorylated protein	+	+	+	+		+	
E	ORF46	UDG	Uracil DNA glucosidase						+	+
L	ORF47	gL	Glycoprotein							
IE	ORF48		Unknown function							
E	ORF49			+	+	+	+	+	+	+
IE	ORF50	RTA	Replication and transcription activator							+
	ORF51		Envelope glycoprotein							
L	ORF52		Virion proteins, unclassified							
L	ORF53	gN	Glycoprotein			+				
E	ORF54		dUTPase						+	+
L	ORF55		Tegument protein						+	+
E	ORF56	PRI	Viral primase, DNA replication protein				+			+
E	ORF57	MTA	M transactivator, posttranscriptional regulator							
L	ORF58		EBV BMRF2 homolog					+		+
E	ORF59	PPF	Polymerase processivity factor		+		+		+	+
E	ORF60	RNR	Ribonucleotide reductase small subunits							+
E	ORF61	RNR	Ribonucleotide reductase large subunits							+
L	ORF62		Capsid		+				+	+
E	ORF63		Viral homolog of human NLRP1							+
E	ORF64		Tegument	+	+	+	+	+	+	+
	ORF65		Capsid		+		+	+	+	+
E	ORF66		NA							+
E	ORF67		Primary envelopment processes							
E	ORF68		Glycoprotein	+	+				+	+
E	ORF69	p33	Primary envelopment processes	+					+	+

(Continued on following page)

TABLE 1 (Continued)

Classification	KSHV ORF	Name	Associated function	Enrichment[a]						
				LANA	RTA	K8	H3K4me3	H3K9me3	H3Ac	H3K27me3
	ORF70		Thymidylate synthase		+		+	+		
L	ORF71/K13	vFLIP	Virus-encoded FLICE-inhibitory proteins							
L	ORF72	vCyclin	Viral cyclin D homolog						+	+
L	ORF73	LANA	Viral tethering, oncogene, etc., as called LANA-1	+	+				+	+
E	ORF74	GPCR	G-protein-coupled receptor							+
	ORF75		Tegument protein/ FGARAT/activator of NF-κB		+					+
	K1	ORF1	Transmembrane glycoprotein K1							
	K10		NA							
L	K10.5	vIRF3	Viral interferon regulatory factor 3 or LANA-2							
	K11.1	vIRF2	Viral interferon regulatory factor 2		+	+				+
L	K12	Kaposin	Oncogene			+				+
	K14		NCAM-like adhesion protein, cytokine							+
	K15		Transmembrane protein, angiogenesis			+		+		+
E	K2	vIL-6	IL-6-like cytokine							
	K3	MIR-1	E3 ubiquitin ligases/ inhibition of IFN-γ and MHC-I	+	+	+	+	+	+	+
E	K4	vMIP-II	Angiogenesis, chemotaxis, cytokine							
	K4.1	vMIP-III	Angiogenesis, chemotaxis, cytokine							
IE/E	K5	MIR-2	E3 ubiquitin ligases/ inhibition of IFN-γ and MHC-I							
E	K6	vMIP-1	Cytokine							+
	K7	vIAP	Viral inhibitor of apoptosis protein							
E	K8	k-bZIP	E3 ubiquitin ligases with specificity toward SUMO2/3			+				
L	K8.1		Glycoprotein							
E	K9	vIRF-1	IFN regulatory factor protein							+

[a] +, enrichment of target more than 2-fold over that obtained from an isotype antibody control from ChIP assay.
[b] Abbreviations: IE, immediate early lytic; E, early lytic; L, latent; HHV-5, human herpesvirus 5; MHV, murine herpesvirus; HRE, hypoxia response element; NA, not available; IL-6, interleukin-6; IFN-γ, gamma interferon.

K8. These domains/clusters are between the genome coordinates 8 and 30 kb, 53 and 80 kb, and 105 and 130 kb, which encompass genes including K3, ORF49, and ORF64 (Fig. 2 and 3). This is reminiscent of what was seen in the results of the H3K4me3, H3K9me3, H3K27me3, and H3Ac ChIP assays (Fig. 1 and 3). The regions which encompass genes for K3, ORF49, and ORF64 showed a distinct enrichment pattern for association with KSHV latent/lytic proteins LANA, RTA, and K8 as well as histone modification proteins during the early stages of KSHV primary infection. Therefore, we hypothesized that these proteins are important for orchestrating the critical events during early infection of PBMCs by KSHV. Here, we focused on 3 genes that were affected, K3, ORF49, and ORF64, because they showed significant changes during PBMC infection and were not extensively explored previously in the physiologically relevant primary cell background PBMCs. We investigated the expression of these three ORFs to further

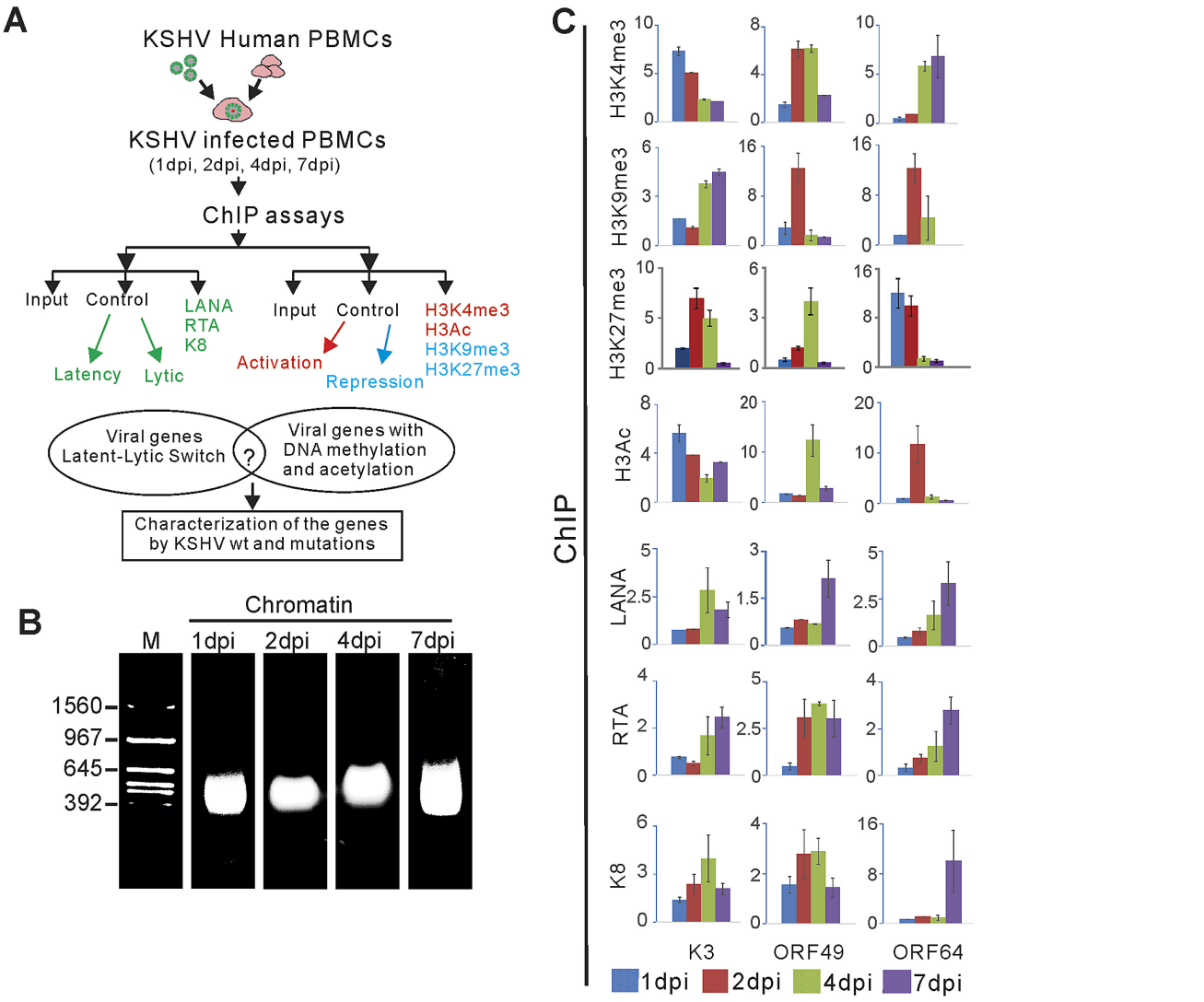

FIG 3 Schematic representation of the experimental setup for genome-wide ChIP analysis during KSHV early primary infection. (A) Experimental flow schematic for ChIP assay during KSHV early primary infection. (B) A representative picture of sonicated DNA samples from KSHV-infected PMBCs at 1, 2, 4, and 7 days p.i. After sonication, 10 μl sonicated DNA samples was run on a 1.5% agarose gel to verify that sonication had resulted in ~500-bp DNA fragments. Numbers at left are sizes in bp. (C) Analysis of histone modification and gene regulation of K3, ORF49, and ORF64 during KSHV primary infection at 1, 2, 4, and 7 days p.i. Human PBMCs were infected by wt KSHV, and cells were harvested at 1, 2, 4, and 7 days p.i. ChIP assays were performed with wt KSHV-infected human PBMCs using the antibodies for histone modification markers (H3K4me3, H3K9me3, H3K37me3, and H3Ac) and KSHV proteins (LANA, RTA, and K8). Real-time quantitative reverse transcription-PCR (qRT-PCR) was performed on a StepOnePlus real-time PCR system. dpi, days postinfection.

explore the mechanism of gene expression at these viral genomic sites during KSHV primary infection. During the first 7 days p.i., these 3 genes, K3, ORF49, and ORF64, showed distinctly different associations with changes in histone modifications and with KSHV latent and lytic antigens (Fig. 3). Interestingly, the H3K4me3 activation mark was highly induced within 24 h after infection but gradually decreased after 48 h and continued up to 7 days p.i. (Fig. 3).

The repressive histone mark H3K9me3 was enriched at the K3 site, increasing up to 7 days p.i., which is in sharp contrast to the activation mark H3K4me3. Moreover, H3K27me3 was enriched after 48 h and was maintained until 4 days p.i. However, the H3Ac modification showed a pattern of enrichment of K3 similar to that of the H3K4me3 activation mark. On further analysis, we showed that LANA as well as RTA association was enriched at K3. However, the b-Zip K8 lytic protein increased steadily up to 4 days p.i. and then declined at 7 days p.i., suggesting a transcriptional role for K8 during early infection of PBMCs by KSHV (Fig. 3). K3 may therefore be involved in the early steps of KSHV infection and is temporally regulated.

Previous studies of ORF49 suggested a role in KSHV lytic replication cooperating with RTA to activate lytic transcription through the c-Jun and p38/Jun N-terminal protein kinase (JNK) pathway (39). Here, we showed that ORF49 was associated with repressive and activation marks on histones which are enriched at 2 days p.i. for repressive H3K9me3 and at 4 days p.i. for H3K4me3 and activation (Fig. 3). Interestingly, by 7 days p.i. the enriched signals for both the activation (H3K4me3) and repressive

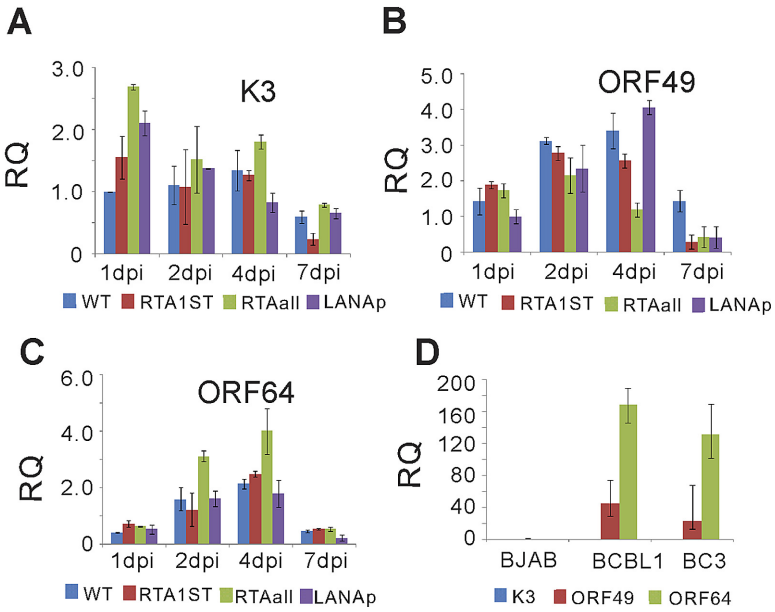

FIG 4 Analysis of mRNA levels for K3, ORF49, and ORF64 during KSHV primary infection at 1, 2, 4, and 7 days p.i. Human PBMCs were infected by wt KSHV, RTA1st, RTA$_{all}$, and LANAp, and cells were harvested at 1, 2, 4, and 7 days p.i. Total RNAs were extracted by using TRIzol (Invitrogen), and cDNAs were synthesized using a high capacity RNA-to-cDNA kit. The mRNA levels of K3 (A), ORF49 (B), and ORF64 (C) were quantified by qRT-PCR on a StepOnePlus real-time PCR system. (D) The mRNA levels of K3, ORF49, and ORF64 in BJAB, BCBL1, and BC3 cells were analyzed by qRT-PCR. dpi, days postinfection; RQ, relative quantity.

(H3K9me3) marks were sharply diminished, suggesting a role for ORF49 and lytic replication at 4 days p.i. (Fig. 3). In this investigation, we demonstrated that the association of LANA, RTA, and K8 at ORF49 was enriched at 2 days p.i. and maintained up to 7 days p.i., although the K8 association was somewhat diminished at that time (Fig. 3).

KSHV-encoded ORF64 is an identified deubiquitination enzyme (Dub) and is important for regulating the activity of the RIG-1 sensor which mediates interferon-induced signaling activity (40, 41). This tegument protein was associated with the H3K4me3 activation marks, which increased up to 7 days p.i., suggesting increased expression of ORF64 up to 7 days p.i. However, a similar increase was seen for enrichment for H3Ac as well as the repressive mark H3K9me3 at 2 days p.i. but was substantially diminished at 4 days p.i. and much more so at 7 days p.i. (Fig. 3). One interesting observation was the association of LANA, RTA, and K8 at increasing levels as seen up to 7 days p.i. (Fig. 3). These data provide new insights into the role of important KSHV-carried genes during the early stages of PBMC infection.

KSHV-carried K3, ORF49, and ORF64 have distinctly different mRNA expression profiles during early infection. In analyzing the data obtained from our ChIP assay focusing on the KSHV genes within the LuR which were associated with KSHV latent/lytic proteins (LANA/RTA/K8) as well as histone modification, we identified a number of virus-carried genes associated with epigenetic modifications in addition to the latent/lytic replication antigens during early primary infections (Table 1).

To further explore the relevance of the histone modifications and the association with latent/lytic replication antigens during early infection, we used recombinant viruses, LANAp (RBP-Jκ binding site deleted within the LANA promoter), RTA1st (first RBP-Jκ binding site deleted within the RTA promoter), and RTA$_{all}$ (all three RBP-Jκ binding sites deleted within the RTA promoter), to infect human PBMCs. These recombinant viruses are important as they can preferentially select latent or lytic replication after infection (22, 23). We monitored the kinetics of mRNA levels of three distinctly different genes, K3, ORF49, and ORF64, in human PBMCs infected with these recombinant viruses at 1, 2, 4, and 7 days p.i. (Fig. 4). The results showed that with the wild-type (wt) KSHV infection, expression of K3 plateaued at 1 day p.i. and continued at that level for up to 4 days p.i. and then showed a slight decline at 7 days p.i. (Fig. 4A). This indicated that K3 is robustly expressed and is likely associated with regulation of critical processes required for KSHV early infection and subsequent persistence of the virus in infected cells. Importantly, PBMCs infected with recombinant virus RTA$_{all}$ (deleted for all three RBP-Jκ sites in the RTA promoter) showed the highest expression of K3 at 1 day p.i. (24 h after infection), which was more than 2-fold over that seen with wt virus. Further, this expression of K3 gradually diminished over 7 days p.i. and was more pronounced with the LANAp recombinant (Fig. 4A). The results therefore suggest that K3 may contribute to the establishment of latency during the early stages of infection (Fig. 4A). K3 expressed very early during KSHV PBMC infection may be critical for the establishment of KSHV within the first 24 h of PBMC infection. In contrast, ORF49 levels continuously increased during KSHV infection of PBMCs up to 4 days p.i. and had a more pronounced expression level in KSHV LANAp-infected PBMCs. This suggests that ORF49 contributed to KSHV early lytic replication programming, as the KSHV LANAp virus is more prominent for driving lytic replication (22) (Fig. 4B). ORF64 gradually increased during KSHV primary PBMC infection and was dramatically enhanced when using the KSHV RTA$_{all}$ recombinant virus with about an 8-fold increase. This suggests that ORF64 most likely contributes to KSHV latent

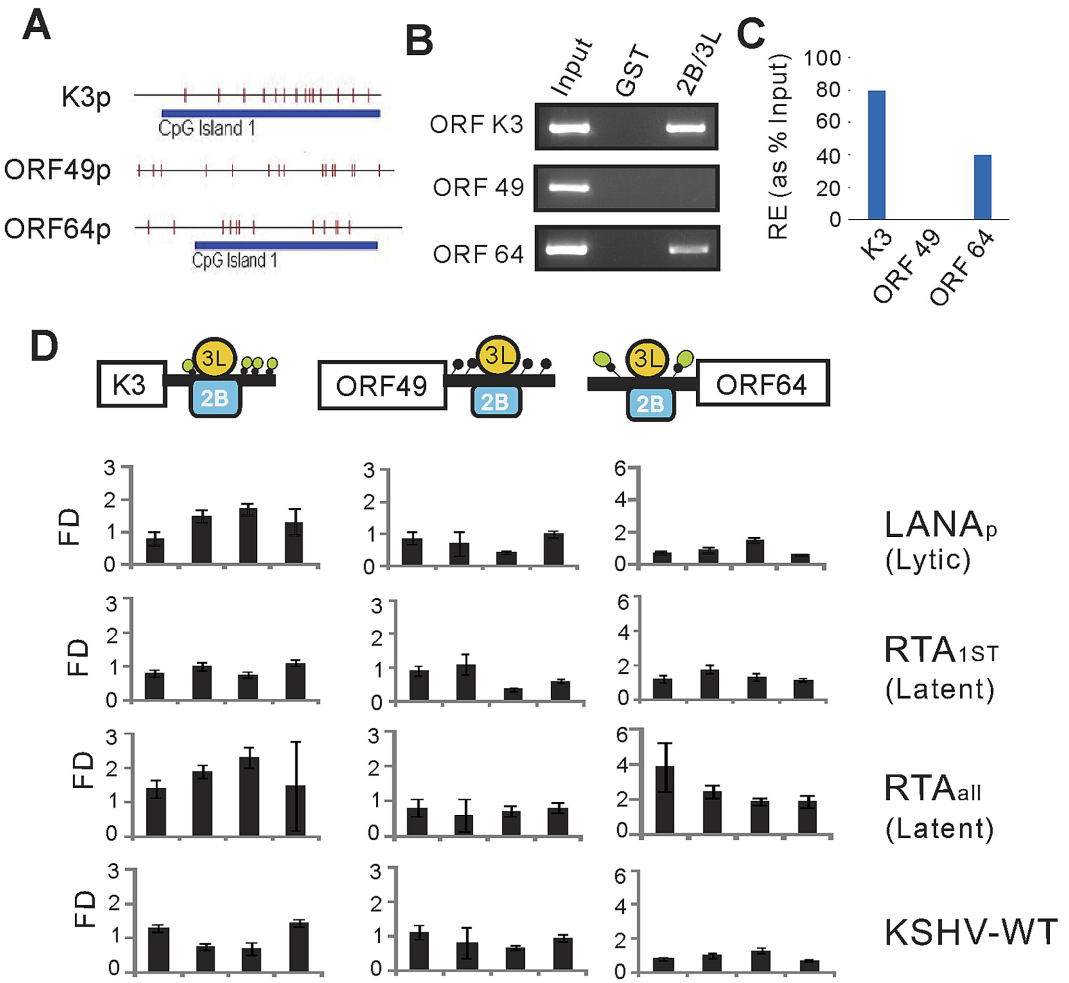

FIG 5 Methylated-CpG island recovery assay (MIRA) utilizes the high enrichment of the MBD2B/MBD3L1 (2B/3L) complex for double-stranded methylated DNA (61). It is able to recover the methylated DNA without the use of bisulfite conversion or antibody recognition and is sensitive enough to detect low-density methylation of a single methylated CpG nucleotide. Analysis of active CpG levels for promoters of K3, ORF49, and ORF64 during KSHV primary infection at 1, 2, 4, and 7 days p.i. (A) The CpG islands within K3, ORF49, and ORF64 promoters were confirmed by Meth Primer software. (B) Relative degree of methylation in KSHV episome from BCBL1 cells examined by MIRA approach. We validated the MIRA using primers across the KSHV K3, ORF49, and ORF64 promoters. (C and D) Human PBMCs were infected by wt KSHV, RTA1st, RTA$_{all}$, and LANAp, and cells were harvested at 1, 2, 4, and 7 days p.i. Samples were sonicated and subjected to MIRA, which utilized the high enrichment of the MBD2B/MBD3L1 complex for double-stranded methylated DNA. The activities of CpG islands within the K3, ORF49, and ORF64 promoters were determined by qRT-PCR. WT, wild type; dpi, days postinfection; FD, fold change in antibody compared to IgG control; RE, relative enrichment.

programming during the early period of PBMC infection (Fig. 4C). Interestingly, ORF64 signals were dramatically reduced at 7 days p.i. after a robust expression at 4 days p.i. (Fig. 4C).

To compare the mRNA levels in latently infected cells to those seen during early infection, we further investigated the mRNA levels of K3, ORF49, and ORF64 in KSHV-latently infected cell lines BCBL1 and BC3. The results showed that K3 had a very low to undetectable level of expression, which corroborated our above findings that K3 may likely function primarily during early infection (Fig. 4D). Because of a low level of spontaneous reactivation in BCBL1 and BC3, as expected we saw active expression of ORF49 in these cell lines (Fig. 4D). However, the tegument protein ORF64 showed a significant level of expression in both cell lines, indicating that ORF64 may also be functioning as an active latent gene, which is annotated as a tegument protein but may also have functions important for latent infection. Taken together, these data suggest that the RBP-Jκ sites within the RTA promoter play critical roles in the establishment of KSHV latent infection.

K3 and ORF64 possess activated CpG islands, which are regulated during the early stages of PBMC infection by KSHV. The KSHV genome is subject to enhanced methylation at CpG dinucleotides (33). CpG DNA methylation is one of the main epigenetic modifications that play an important role in the control of gene expression (42). Recently, parvovirus B19 DNA was reported to become methylated at CpG sites during *in vitro* infection (43). Additionally, two methylated CpG islands flank the HIV-1 transcription start site and contribute to regulation of HIV latency in infected Jurkat and primary CD4$^+$ T cells (44). Our data showed that many ORFs, such as K3, ORF49, and ORF64, may possess "bivalent" chromatin within their promoter (Fig. 5 and Table 1). Thus, we speculated that CpG islands, which may function to subtly regulate gene expression, could determine the overall out-

come of KSHV infection. Our results computationally indicated that these activated genes possess CpG islands by Meth Primer software (Fig. 5A). Investigation of activated CpG islands is likely to further elucidate the gene expression changes of KSHV during the early stages of primary infection. To identify the CpG islands responsible for modulation of KSHV gene expression, we recently developed a methylated-CpG island recovery assay (MIRA) (Fig. 5A). We confirmed that both K3 and ORF64 contained activated CpG islands within their promoters. However, ORF49 showed a minimal CpG island footprint within its promoter as seen by the methyl CpG binding protein 2B/3L assay (Fig. 5B), indicating that ORF49 might have atypical CpG islands within its promoter, consistent with the computational prediction (Fig. 5A). We further compared the methylated statuses of these promoters, K3, ORF49, and ORF64, at 1, 2, 4, and 7 days p.i. to examine the activity of the CpG islands during primary infection by using the KSHV wt, LANAp, RTA1st, and RTA$_{all}$ recombinant viruses. Our results showed that the CpG islands at the K3 promoter possessed activated CpG islands as early as 1 day p.i. during primary infection, and both the RTAp recombinant viruses showed that the K3 promoter also had highly activated CpG islands by 2 days p.i. which plateaued at 4 days p.i. (Fig. 5A, B, and C). These results suggest that K3 is active during initial infection and that the activated CpG islands are then suppressed by 7 days p.i. In contrast, ORF64 showed a gradual decrease in CpG methylation from 1 day p.i. to 7 days p.i. for the RTA$_{all}$ recombinant, which suggests that ORF64, if expressed early, may induce lytic replication during the early stages of primary infection as the RTA$_{all}$ recombinant is driven toward a latent-type replication cycle. However, the low CpG activities which declined after 24 h most likely regulate the infection by allowing abundant mRNA expression of ORF64 and thus contributing to the establishment and maintenance of KSHV latent infection (Fig. 5A and D).

The KSHV genome contains bivalent chromatin during the early stages of PBMC infection. The above epigenetic changes showed that the KSHV genome is dynamically modified during early PBMC infection. Previous studies have shown that the RTA promoter possesses a distinct bivalent promoter during lytic replication (32, 33). Our results demonstrated that K3 as well as ORF64 showed different patterns in terms of its mRNA expression, histone modification, and CpG activation. Though the ORF49 promoter may not have the typical CpG islands, the ChIP assay showed that ORF49 was enriched for histone modification. We postulated that K3, ORF49, and ORF64 may contain bivalent chromatin important for the dynamic regulation of their expression during the early stages of primary infection. We investigated whether K3, ORF49, and ORF64 possessed bivalent chromatin across their promoters during primary infection. H3K4me3 was used as an active marker and H3K27me3 was used as a repressive marker to monitor the changes within these promoters. The precipitated ChIP DNAs were measured by qPCR, using specific primers from the promoter regions of K3, ORF49, and ORF64 (Fig. 6A and C). The results showed that K3 and ORF64 had bivalent chromatin domains as defined by the concomitant presence of the activating H3K4me3 and the repressive H3K27me3 signals (Fig. 6A and C). However, the K3 promoter showed the strongest enrichment for H3K4me3 at 2 days p.i., which was repressed by 4 days p.i. and continued to decrease until 7 days p.i. for H3K27me3 (Fig. 6A). In contrast, ORF64 showed the highest enrichment for H3K4me3 at 4 and 7 days p.i. compared to H3K27me3 at 1 and 7 days p.i. (Fig. 6C). These results provide an explanation as to why KSHV-carried K3 may be expressed as an immediate early gene during KSHV primary infection with related functions but why ORF64 is likely to be a critical gene required for the establishment and maintenance of KSHV latent infection through regulation of the antiviral response at the early stages of primary infection. Surprisingly, antibodies against H3K4me3 and H3K27me3 simultaneously bound the ORF49 promoter from 1 day to 7 days p.i., suggesting that ORF49 may have a bivalent chromatin structure, which regulates ORF49 expression during primary infection. Noticeably, the ORF49 promoter was gradually enriched for H3K4me3, increasing to 2 and 4 days p.i. However, this enrichment was dramatically reduced by 7 days p.i. Furthermore, we observed a striking increase in H3K27me3 at 1 day p.i., which was dominant at 7 days p.i., although with a drop in about 55% enrichment (Fig. 6B). The studies showed that KSHV might utilize bivalent chromatin to dynamically regulate gene expression during its early infection of human primary cells.

DISCUSSION

KSHV is found in immunoblastic B cells of HIV patients with multicentric Castleman's disease (MCD) and, predominantly in a latent form, in primary effusion lymphoma (PEL) cells and Kaposi's sarcoma (KS) spindle cells (45). The early period of infection for KSHV is a dynamic process, involving the collaboration of many viral genes, which are temporally and epigenetically regulated. Therefore, understanding the changes in the KSHV genome during the early stages of infection will provide clues to the mechanism regulating this period of KSHV infection in human PBMCs and development of KSHV-associated B cell-lymphoma. Furthermore, infection of PBMCs is likely an important, if not critical, part in the ability of the virus to gain access to the human host.

Viral infection by KSHV initially triggers activation of a subset of genes as well as inducing chromatin modifications. Studies have shown that Marek's disease virus (MDV) infection induces widespread differential chromatin marks in inbred chicken lines (46). Epstein-Barr virus (EBV) also induces epigenetic alterations following transient infection (47). Further, KSHV experiences unique epigenetic modifications across the whole genome during latent and lytic replication, as well as during early infection in epithelial cells (32, 33). Here, our investigation showed that histone modifications across the KSHV genome presented a unique pattern of histone modifications (H3K4me3, H3K9me3, H3K27me3, and H3Ac) during early infection of human PBMCs. The histone modifications were exhibited in a temporal manner, which suggested that KSHV early infection is a dynamic process. It was noteworthy that the majority of the epigenetic modifications were suppressed at 7 days p.i., which strongly suggested that those early epigenetic modifications were crucial to the successful establishment of latent infection in B cells post-infection of PBMCs and that infection of T cells may also be critical to the changes and persistence of the virus in the B-cell compartment.

Previous studies investigating KSHV latent/lytic genes and genome-wide epigenetic modifications were focused on KSHV-latently infected B-lymphoma and epithelial cell lines (32, 33, 38). Our studies further showed that the KSHV latent genes, as well as a subset of lytic genes, were tightly regulated during early primary infection of human PBMCs. Furthermore, it was surprising that the genes regulated by the KSHV major lytic transactivators were different from those seen in latently infected cell lines (48). These

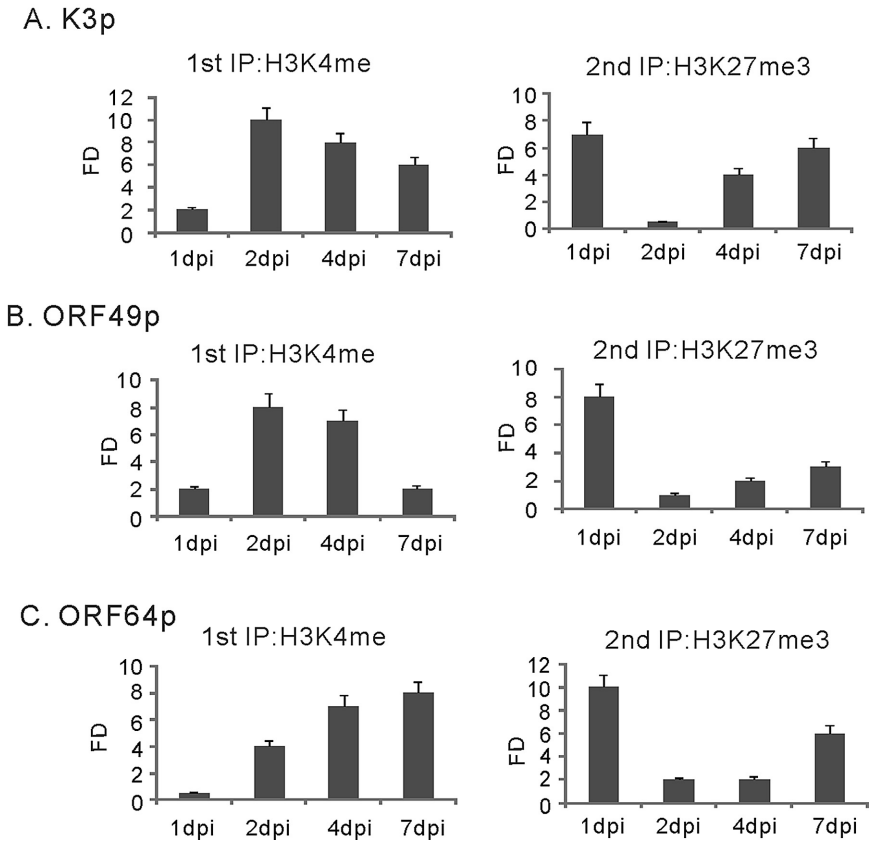

FIG 6 Bivalent histone modification patterns at K3, ORF49, and ORF64 promoters. Sequential ChIP assays were performed with antibodies directed against H3K4me3 and H3K27me3 during the first and second rounds of immunoprecipitation (IP). (A) K3 promoter. (B) ORF49 promoter. (C) ORF64 promoter. FD, fold change in antibody compared to IgG control.

results suggest that KSHV utilizes a novel programming strategy to successfully transit through the early stages of human PBMC infection. The data further showed that KSHV-carried K8 played a critical role in triggering viral lytic replication during the early period of PBMC infection. Notably, the regulated genes were dramatically activated at 7 days p.i. so that a fully lytic cycle was induced and virion particles were released. This explains why a large fraction of the population of KSHV-infected PBMCs were lysed after 7 days p.i. In addition, the activation or suppression of specific KSHV transcripts further underscores the complexity of these regulatory events and helps to illuminate the early events during KSHV infection, which shows temporal regulation of specific genes during this infection period.

We have now shown that a number of KSHV genes, which include K3, ORF49, and ORF64, were not previously identified as latent or lytic genes and were temporally activated or repressed during primary infection. KSHV-carried K3 is a homolog of the membrane-associated RING-CH (MARCH) E3 ubiquitin ligase gene family and was detected as one of the lytic replication genes (49). K3 also contributes to downregulation of major histocompatibility complex class I (MHC-I) surface expression (50). However, recent studies showed that deletion of K3 does not restore MHC-I expression during lytic replication, suggesting that other KSHV antigens could be involved (51). K3 was also activated and expressed earlier than were ORF49 and ORF64 during the early period of PBMC infection. K3 transcripts were induced very early upon virus reactivation in PEL cells (52). Therefore, K3 may function as an immediate early gene product important for regulating KSHV early lytic infection. KSHV-carried ORF49 is an immediate early gene during the KSHV lytic cycle. It is located adjacent to and in the opposite orientation from the immediate early replication and transcription activator for Rta/ORF50 (39). It shares some part of the promoter with ORF50, which possesses active CpG islands (33). Our data showed that the promoter of ORF49 (~200 bp) does not contain a typical activated CpG island. However, it is also important to note that CpG methylation of KSHV DNA in tumor cell lines or in infected endothelial cells has been consistently reported (32, 33), whereas DNA extracted from virions does not show CpG methylation (33). Though KSHV early infection showed profound changes in methylation status across the viral genome, our data further demonstrate that a subset of genes, which include K3 and ORF64, have distinct activated CpG islands as determined by MIRA in KSHV-infected human PBMCs. This is also consistent with data that show that ORF64 was amplified from methyl-CpG binding domain 2 (MBD2) beads which immunoprecipitated KSHV viral DNA in KSHV-latently infected BC3 cells (53). Further studies to identify specific cytosine methylation within these viral ORFs using bisulfate sequencing are ongoing. Further consideration also needs to be given to infection of T cells from the PBMC population. B cells and other cells are infected with KSHV and may exhibit rather different cytosine methylation at these ORFs, although this is un-

likely to be the case during early infection. This is more likely to be so after 7 days p.i. for establishment of latency. However, our results did show that changes at the KSHV genome occurred during KSHV early primary infection. These profiles of KSHV CpG methylation at early stages of primary infection could be utilized to monitor KSHV early infection and transmission in patients.

Early detection of KSHV infection is important for the prevention and treatment of KSHV-associated lymphoproliferative disorder. Recently, a study showed that early childhood infection by KSHV is highly prevalent in Zambian children (54). Molecular analysis has showed that KSHV may possess a variant strain during viral transmission between children and adults (51). Furthermore, the virus may exist in different stages or phases of latency based on the genetic background or cancer phenotype, similarly to what has been demonstrated for EBV-associated cancers. Therefore, early detection for KSHV infection in the blood cells of children will help in monitoring KSHV infection and its transmission (51). K3, ORF49, and ORF64 exhibit different profiles during the early stage of infection in PBMCs. Therefore, these could be utilized as potential biomarkers for the detection of KSHV during early infection of human blood lymphocytes. These studies provide further clues to a deeper understanding of the early process of KSHV infection in human PBMCs and may also have some benefit in clinical detection of KSHV in HIV-positive patients who may be at risk for developing pleural effusion lymphomas.

MATERIALS AND METHODS

Bioethics statement. Deidentified total human peripheral blood mononuclear cells (PBMCs) were obtained from the University of Pennsylvania Human Immunology Core (HIC). The HIC maintains the institutional review board (IRB)-approved protocols according to which Declaration of Helsinki protocols were followed and each donor/patient gave written, informed consent.

Cells, BACmid, and antibodies. The wild-type KSHV BACmid, BAC36 wt, was provided by S. J. Gao (University of Texas, San Antonio, TX) (55). BACmid mutations, BACLANAp, RTA1st, and RTA$_{all}$, were as described previously (56). Antibodies against LANA and RTA are purified ascites from mouse injected by hybridoma from Ke Lan, Institute Pasteur of Shanghai (Shanghai, China). The K8 antibody was a kind gift from Yuan Yan (School of Dental Medicine, University of Pennsylvania). Antibodies against H3K4me3 (Millipore 07-473), H3K9me3 (Millipore 07-442), H3K27me3 (Cell Signaling C36B11), and H3Ac (Millipore 06-599) were used for histone modifications.

Chromatin immunoprecipitation assay. PBMCs (40×10^6 to ~50×10^6) were infected by incubation with virus suspension for 1, 2, 4, and 7 days (22, 23). Cells from these fractions were cross-linked with 1% (vol/vol) formaldehyde for 10 min followed by addition of 125 mM glycine for 5 min to stop the cross-linking reaction (57). Nuclei from these cells were isolated, followed by sonication of the chromatin to an average length of 500 bp. Samples were precleared with salmon sperm DNA/protein A Sepharose slurry for 30 min at 4°C with rotation. Supernatants were collected after brief centrifugation. A 20% portion of the total chromatin sample was set aside for the later preparation of input controls. The remainder, 80%, was subjected to immunoprecipitation using 5 μg of control serum and corresponding antibodies. The remainder was divided into two fractions, (i) control serum (Sigma-Aldrich, St. Louis, MO) and (ii) antibodies specific for KSHV latent and lytic protein and histone modifications. Immune complex was precipitated using salmon sperm DNA and protein A+G slurry. Beads were then washed and eluted by using the elution buffer (1% SDS, 0.1 M $NaHCO_3$) and reverse cross-linked by adding 0.3 M NaCl at 65°C for 4 to 5 h. The eluted DNA was purified by treatment with proteinase K at 45°C for 2 h; phenol extraction and ethanol precipitation were carried out. Chromatin saved for input was also reverse cross-linked to extract DNA for real-time PCR analysis. Purified DNA was dissolved in 100 μl sterile water and stored at −20°C.

Sequential ChIP. Sequential ChIP was employed to detect the colocalization of bivalent histone marks. The first ChIP assay was performed as described above. The immunoprecipitated DNA/protein complexes were treated as described previously (32). Ten percent of eluted DNA/protein complexes was saved and diluted in 1 ml ChIP dilute buffer (0.01% SDS, 1.1% Triton X-100, 1.2 mM EDTA, 16.7 mM Tris, pH 8.1, 167 mM NaCl plus protease inhibitors), the second ChIP was performed as described above, the purified DNAs were analyzed by qPCR, and the enrichment of the histone modifications on specific genomic regions was calculated as a percentage of the immunoprecipitated DNA compared to the total amount of DNA eluted after the first ChIP.

qPCR. The quantitative real-time PCR (qPCR) was performed on a StepOnePlus real-time PCR system (Applied Biosystems Inc., Carlsbad, CA) using Power SYBR green PCR master mix (Applied Biosystems Inc., Carlsbad, CA) as described earlier (58, 59). The reactions were carried out in a 96-well plate at 95°C for 10 min, followed by 40 cycles at 95°C for 30 s, 52°C for 30 s, and then 72°C for 30 s. Primers spanning the entire KSHV genome at every 1.5 kb were used in the real-time PCR assay (see Table S1 in the supplemental material). Relative amounts of DNA bound in chromatin were calculated by subtracting the amplification with control antibody.

RNA extraction and RT-PCR. Total RNAs from infected PBMCs were extracted by using TRIzol (Invitrogen, Inc., Carlsbad, CA), and 1.0 μg DNase-treated total RNA was used to generate cDNA using the high capacity RNA-to-cDNA kit (Applied Biosystems Inc., Foster City, CA) according to the manufacturer's instructions. Reverse transcription-PCR (RT-PCR) was performed on a StepOnePlus real-time PCR system (Applied Biosystems Inc., Carlsbad, CA) or Opticon 2 real-time PCR system. The reactions were carried out in a 96-well plate at 95°C for 10 min, followed by 40 cycles at 95°C for 30 s, 52°C for 30 s, and then 72°C for 30 s. The differences in cycle threshold values (C_T) between the samples (ΔC_T) were calculated after standardization by glyceraldehyde-3-phosphate dehydrogenase (GAPDH) and converted to fold changes using one of the samples as a standard (1-fold). The primers used were as follows: K3 (5′ GGCCGTGTTTCTAGAGATAGTG 3′ and 5′ GGGACCCCGGTTGCCTGGAC 3′), ORF49 (5′ ACTGAAAGGAGGGAGCACAC 3′ and 5′ GCTGCATAGGTTTTGAGAGA 3′), ORF64 (5′ CTGGCCTCACGCACCTGCAG 3′ and 5′ TAACACTGGAATTGATACGG 3′), and GAPDH (5′ GGTCTACATGGCAACTGTGA 3′ and 5′ ACGACCACTTTGTCAAGCTC 3′). All the reactions were run in triplicate.

MIRA. Methyl-CpG binding domain protein 2B (MBD2B) and the methyl-CpG binding domain protein 3-like 1 (MBD3L1) were cloned into pGEX-5X1 and pET28a (+) vectors and confirmed by DNA sequencing. pGEX-5X1-MBD2B and pET28a (+)-MBD3L1 were transfected into BL21 cells and expressed at 30°C overnight after induction. Glutathione *S*-transferase (GST) proteins were purified, and effectiveness was verified by using specific KSHV primers. Methylated-CpG island recovery assays (MIRAs) were performed as essentially described previously (60). Briefly, sonicated KSHV-infected PBMC samples were precleared with GST beads for 2 h. Then, 1 μg purified GST-tagged MBD2B and 1 μg purified His-tagged MBD3L1 were combined to immunoprecipitate the sonicated DNA/protein complexes from KSHV-infected PBMCs for 4 h at 4°C with continuous rotation. Immunoprecipitated DNA/protein complexes were washed 3 times with washing buffer (10 mM Tris-HCl [pH 7.5], 700 mM NaCl, 1 mmol/liter EDTA, 1 mM dithiothreitol [DTT], 3 mM $MgCl_2$, 0.1% Triton X-100, 5% glycerol, 25 μg/ml bovine serum albumin) and were resuspended in 100 μl of elution buffer for incubation at 50°C for 1 h. Pellets were removed by centrifugation at 800 rpm for 5 min, the supernatant was transferred into a new tube, and DNA fragments were precipitated by 100% ethanol with subsequent extraction in phenol-chloroform-isopropanol. Activated CpG islands within KSHV K3, ORF49, and ORF64 promoter regions were detected by using the following primer sets: K3, 5′ CTCCTCGTTGCAAATCCAGC 3′ and 5′ CTGA

GCCACAAACGCCCCTC 3′; ORF49, 5′ TAAACAGATGGTTGAACAG GTG 3′ and 5′ GAAAAAAGCAGAAAAGGTTAAAC 3′; and ORF64, 5′ G GGACAACGGCAGGGGGCGGC 3′ and 5′ ATACAGTTAGCTTGGTG GGTG 3′.

SUPPLEMENTAL MATERIAL

Supplemental material for this article may be found at http://mbio.asm.org/lookup/suppl/doi:10.1128/mBio.02261-14/-/DCSupplemental.

Table S1, DOCX file, 0.1 MB

ACKNOWLEDGMENTS

We thank Yuan Yan (Department of Microbiology, University of Pennsylvania School of Dental Medicine) for K8 antibody and Ke Lan (Institute Pasteur of Shanghai, Chinese Academy of Sciences) for LANA antibody. We thank the Human Immunology Core at the University of Pennsylvania for isolating PBMCs, and anonymous blood donors. We are grateful to Paul Lieberman for advice in doing ChIP assays for epigenetic analysis. We are also grateful to Santosh Upadhyay for making the pGEX-5×1-MBD2b and pET28a (+)-MBD3L1 constructs.

This work was supported by Public Health Service grants P01-CA-174439, R01-CA-137894, R01-CA-171979, R01-CA-1744301, P30-DK-050306, and R01-CA-177439 (to E.S.R.).

REFERENCES

1. **Cesarman E, Chang Y, Moore PS, Said JW, Knowles DM.** 1995. Kaposi's sarcoma-associated herpesvirus-like DNA sequences in AIDS-related body-cavity-based lymphomas. N. Engl. J. Med. **332:**1186–1191. http://dx.doi.org/10.1056/NEJM199505043321802.
2. **Moore PS, Chang Y.** 1995. Detection of herpesvirus-like DNA sequences in Kaposi's sarcoma in patients with and without HIV infection. N. Engl. J. Med. **332:**1181–1185. http://dx.doi.org/10.1056/NEJM199505043321801.
3. **Soulier J, Grollet L, Oksenhendler E, Cacoub P, Cazals-Hatem D, Babinet P, d'Agay MF, Clauvel JP, Raphael M, Degos L, Sigaux F.** 1995. Kaposi's sarcoma-associated herpesvirus-like DNA sequences in multicentric Castleman's disease. Blood **86:**1276–1280.
4. **Rettig MB, Ma HJ, Vescio RA, Pold M, Schiller G, Belson D, Savage A, Nishikubo C, Wu C, Fraser J, Said JW, Berenson JR.** 1997. Kaposi's sarcoma-associated herpesvirus infection of bone marrow dendritic cells from multiple myeloma patients. Science **276:**1851–1854. http://dx.doi.org/10.1126/science.276.5320.1851.
5. **Chang Y, Cesarman E, Pessin MS, Lee F, Culpepper J, Knowles DM, Moore PS.** 1994. Identification of herpesvirus-like DNA sequences in AIDS-associated Kaposi's sarcoma. Science **266:**1865–1869. http://dx.doi.org/10.1126/science.7997879.
6. **Schulz TF.** 1999. Epidemiology of Kaposi's sarcoma-associated herpesvirus/human herpesvirus 8. Adv. Cancer Res. **76:**121–160. http://dx.doi.org/10.1016/S0065-230X(08)60775-7.
7. **Biggar RJ, Whitby D, Marshall V, Linhares AC, Black F.** 2000. Human herpesvirus 8 in Brazilian Amerindians: a hyperendemic population with a new subtype. J. Infect. Dis. **181:**1562–1568. http://dx.doi.org/10.1086/315456.
8. **Dukers NH, Rezza G.** 2003. Human herpesvirus 8 epidemiology: what we do and do not know. AIDS **17:**1717–1730. http://dx.doi.org/10.1097/00002030-200308150-00001.
9. **Komanduri KV, Luce JA, McGrath MS, Herndier BG, Ng VL.** 1996. The natural history and molecular heterogeneity of HIV-associated primary malignant lymphomatous effusions. J. Acquir. Immune Defic. Syndr. Hum. Retrovirol. **13:**215–226. http://dx.doi.org/10.1097/00042560-199600001-00032.
10. **Polizzotto MN, Uldrick TS, Hu D, Yarchoan R.** 2012. Clinical manifestations of Kaposi sarcoma herpesvirus lytic activation: multicentric Castleman disease (KSHV-MCD) and the KSHV inflammatory cytokine syndrome. Front. Microbiol. **3:**73. http://dx.doi.org/10.3389/fmicb.2012.00073.
11. **Schulte KM, Talat N.** 2010. Castleman's disease—a two compartment model of HHV8 infection. Nat. Rev. Clin. Oncol. **7:**533–543. http://dx.doi.org/10.1038/nrclinonc.2010.103.
12. **Chakraborty S, Veettil MV, Chandran B.** 2012. Kaposi's sarcoma associated herpesvirus entry into target cells. Front. Microbiol. **3:**6. http://dx.doi.org/10.3389/fmicb.2012.00006.
13. **Chandran B.** 2010. Early events in Kaposi's sarcoma-associated herpesvirus infection of target cells. J. Virol. **84:**2188–2199. http://dx.doi.org/10.1128/JVI.01334-09.
14. **Bottero V, Chakraborty S, Chandran B.** 2012. Reactive oxygen species (ROS) are induced by Kaposi's sarcoma-associated herpesvirus early during primary infection of endothelial cells to promote virus entry. J. Virol. **87:**1733–1749. http://dx.doi.org/10.1128/JVI.02958-12.
15. **Ballon G, Chen K, Perez R, Tam W, Cesarman E.** 2011. Kaposi sarcoma herpesvirus (KSHV) vFLIP oncoprotein induces B cell transdifferentiation and tumorigenesis in mice. J. Clin. Invest. **121:**1141–1153. http://dx.doi.org/10.1172/JCI44417.
16. **Hassman LM, Ellison TJ, Kedes DH.** 2011. KSHV infects a subset of human tonsillar B cells, driving proliferation and plasmablast differentiation. J. Clin. Invest. **121:**752–768. http://dx.doi.org/10.1172/JCI44185.
17. **Myoung J, Ganem D.** 2011. Active lytic infection of human primary tonsillar B cells by KSHV and its noncytolytic control by activated CD4+ T cells. J. Clin. Invest. **121:**1130–1140. http://dx.doi.org/10.1172/JCI43755.
18. **Myoung J, Ganem D.** 2011. Infection of primary human tonsillar lymphoid cells by KSHV reveals frequent but abortive infection of T cells. Virology **413:**1–11. http://dx.doi.org/10.1016/j.virol.2010.12.036.
19. **Lan K, Kuppers DA, Robertson ES.** 2005. Kaposi's sarcoma-associated herpesvirus reactivation is regulated by interaction of latency-associated nuclear antigen with recombination signal sequence-binding protein Jkappa, the major downstream effector of the Notch signaling pathway. J. Virol. **79:**3468–3478. http://dx.doi.org/10.1128/JVI.79.6.3468-3478.2005.
20. **Lan K, Kuppers DA, Verma SC, Robertson ES.** 2004. Kaposi's sarcoma-associated herpesvirus-encoded latency-associated nuclear antigen inhibits lytic replication by targeting Rta: a potential mechanism for virus-mediated control of latency. J. Virol. **78:**6585–6594. http://dx.doi.org/10.1128/JVI.78.12.6585-6594.2004.
21. **Lan K, Kuppers DA, Verma SC, Sharma N, Murakami M, Robertson ES.** 2005. Induction of Kaposi's sarcoma-associated herpesvirus latency-associated nuclear antigen by the lytic transactivator RTA: a novel mechanism for establishment of latency. J. Virol. **79:**7453–7465. http://dx.doi.org/10.1128/JVI.79.12.7453-7465.2005.
22. **Lu J, Verma SC, Cai Q, Robertson ES.** 2011. The single RBP-Jkappa site within the LANA promoter is crucial for establishing Kaposi's sarcoma-associated herpesvirus latency during primary infection. J. Virol. **85:**6148–6161. http://dx.doi.org/10.1128/JVI.02608-10.
23. **Lu J, Verma SC, Cai Q, Saha A, Dzeng RK, Robertson ES.** 2012. The RBP-Jkappa binding sites within the RTA promoter regulate KSHV latent infection and cell proliferation. PLoS Pathog. **8:**e1002479.
24. **Jaenisch R, Bird A.** 2003. Epigenetic regulation of gene expression: how the genome integrates intrinsic and environmental signals. Nat. Genet. **33**(Suppl):245–254. http://dx.doi.org/10.1038/ng1089.
25. **Skinner MK, Manikkam M, Guerrero-Bosagna C.** 2010. Epigenetic transgenerational actions of environmental factors in disease etiology. Trends Endocrinol. Metab. **21:**214–222. http://dx.doi.org/10.1016/j.tem.2009.12.007.
26. **Sharma S, Kelly TK, Jones PA.** 2010. Epigenetics in cancer. Carcinogenesis **31:**27–36. http://dx.doi.org/10.1093/carcin/bgp220.
27. **Esteller M.** 2002. CpG island hypermethylation and tumor suppressor genes: a booming present, a brighter future. Oncogene **21:**5427–5440. http://dx.doi.org/10.1038/sj.onc.1205600.
28. **Spivakov M, Fisher AG.** 2007. Epigenetic signatures of stem-cell identity. Nat. Rev. Genet. **8:**263–271. http://dx.doi.org/10.1038/nrg2046.
29. **Esteller M.** 2007. Cancer epigenomics: DNA methylomes and histone-modification maps. Nat. Rev. Genet. **8:**286–298. http://dx.doi.org/10.1038/nrg2005.
30. **Lu F, Stedman W, Yousef M, Renne R, Lieberman PM.** 2010. Epigenetic regulation of Kaposi's sarcoma-associated herpesvirus latency by virus-encoded microRNAs that target Rta and the cellular Rbl2-DNMT pathway. J. Virol. **84:**2697–2706. http://dx.doi.org/10.1128/JVI.01997-09.
31. **He M, Zhang W, Bakken T, Schutten M, Toth Z, Jung JU, Gill P, Cannon M, Gao SJ.** 2012. Cancer angiogenesis induced by Kaposi sarcoma-associated herpesvirus is mediated by EZH2. Cancer Res. **72:**3582–3592. http://dx.doi.org/10.1158/1538-7445.AM2012-3582.
32. **Toth Z, Maglinte DT, Lee SH, Lee HR, Wong LY, Brulois KF, Lee S, Buckley JD, Laird PW, Marquez VE, Jung JU.** 2010. Epigenetic analysis

of KSHV latent and lytic genomes. PLoS Pathog. **6:**e1001013. http://dx.doi.org/10.1371/journal.ppat.1001013.
33. **Günther T, Grundhoff A.** 2010. The epigenetic landscape of latent Kaposi sarcoma-associated herpesvirus genomes. PLoS Pathog. **6:**e1000935. http://dx.doi.org/10.1371/journal.ppat.1000935.
34. **Russo JJ, Bohenzky RA, Chien MC, Chen J, Yan M, Maddalena D, Parry JP, Peruzzi D, Edelman IS, Chang Y, Moore PS.** 1996. Nucleotide sequence of the Kaposi sarcoma-associated herpesvirus (HHV8). Proc. Natl. Acad. Sci. U. S. A. **93:**14862–14867. http://dx.doi.org/10.1073/pnas.93.25.14862.
35. **Grundhoff A, Ganem D.** 2004. Inefficient establishment of KSHV latency suggests an additional role for continued lytic replication in Kaposi sarcoma pathogenesis. J. Clin. Invest. **113:**124–136. http://dx.doi.org/10.1172/JCI200417803.
36. **Krishnan HH, Naranatt PP, Smith MS, Zeng L, Bloomer C, Chandran B.** 2004. Concurrent expression of latent and a limited number of lytic genes with immune modulation and antiapoptotic function by Kaposi's sarcoma-associated herpesvirus early during infection of primary endothelial and fibroblast cells and subsequent decline of lytic gene expression. J. Virol. **78:**3601–3620. http://dx.doi.org/10.1128/JVI.78.7.3601-3620.2004.
37. **Lu F, Tsai K, Chen HS, Wikramasinghe P, Davuluri RV, Showe L, Domsic J, Marmorstein R, Lieberman PM.** 2012. Identification of host-chromosome binding sites and candidate gene targets for Kaposi's sarcoma-associated herpesvirus LANA. J. Virol. **86:**5752–5762. http://dx.doi.org/10.1128/JVI.07216-11.
38. **Chen J, Ye F, Xie J, Kuhne K, Gao SJ.** 2009. Genome-wide identification of binding sites for Kaposi's sarcoma-associated herpesvirus lytic switch protein, RTA. Virology **386:**290–302. http://dx.doi.org/10.1016/j.virol.2009.01.031.
39. **González CM, Wong EL, Bowser BS, Hong GK, Kenney S, Damania B.** 2006. Identification and characterization of the Orf49 protein of Kaposi's sarcoma-associated herpesvirus. J. Virol. **80:**3062–3070. http://dx.doi.org/10.1128/JVI.80.6.3062-3070.2006.
40. **Inn KS, Lee SH, Rathbun JY, Wong LY, Toth Z, Machida K, Ou JH, Jung JU.** 2011. Inhibition of RIG-I-mediated signaling by Kaposi's sarcoma-associated herpesvirus-encoded deubiquitinase ORF64. J. Virol. **85:**10899–10904. http://dx.doi.org/10.1128/JVI.00690-11.
41. **González CM, Wang L, Damania B.** 2009. Kaposi's sarcoma-associated herpesvirus encodes a viral deubiquitinase. J. Virol. **83:**10224–10233. http://dx.doi.org/10.1128/JVI.00589-09.
42. **Iqbal K, Jin SG, Pfeifer GP, Szabó PE.** 2011. Reprogramming of the paternal genome upon fertilization involves genome-wide oxidation of 5-methylcytosine. Proc. Natl. Acad. Sci. U. S. A. **108:**3642–3647. http://dx.doi.org/10.1073/pnas.1014033108.
43. **Bonvicini F, Manaresi E, Di Furio F, De Falco L, Gallinella G.** 2012. Parvovirus b19 DNA CpG dinucleotide methylation and epigenetic regulation of viral expression. PLoS One **7:**e33316. http://dx.doi.org/10.1371/journal.pone.0033316.
44. **Kauder SE, Bosque A, Lindqvist A, Planelles V, Verdin E.** 2009. Epigenetic regulation of HIV-1 latency by cytosine methylation. PLoS Pathog. **5:**e1000495. http://dx.doi.org/10.1371/journal.ppat.1000495.
45. **Ablashi DV, Chatlynne LG, Whitman JE, Jr, Cesarman E.** 2002. Spectrum of Kaposi's sarcoma-associated herpesvirus, or human herpesvirus 8, diseases. Clin. Microbiol. Rev. **15:**439–464. http://dx.doi.org/10.1128/CMR.15.3.439-464.2002.
46. **Mitra A, Luo J, Zhang H, Cui K, Zhao K, Song J.** 2012. Marek's disease virus infection induces widespread differential chromatin marks in inbred chicken lines. BMC Genomics **13:**557. http://dx.doi.org/10.1186/1471-2164-13-557.
47. **Queen KJ, Shi M, Zhang F, Cvek U, Scott RS.** 2013. Epstein-Barr virus-induced epigenetic alterations following transient infection. Int. J. Cancer **132:**2076–2086. http://dx.doi.org/10.1002/ijc.27893.
48. **Nakamura H, Lu M, Gwack Y, Souvlis J, Zeichner SL, Jung JU.** 2003. Global changes in Kaposi's sarcoma-associated virus gene expression patterns following expression of a tetracycline-inducible Rta transactivator. J. Virol. **77:**4205–4220. http://dx.doi.org/10.1128/JVI.77.7.4205-4220.2003.
49. **Dodd RB, Allen MD, Brown SE, Sanderson CM, Duncan LM, Lehner PJ, Bycroft M, Read RJ.** 2004. Solution structure of the Kaposi's sarcoma-associated herpesvirus K3 N-terminal domain reveals a novel E2-binding C4HC3-type RING domain. J. Biol. Chem. **279:**53840–53847. http://dx.doi.org/10.1074/jbc.M409662200.
50. **Ishido S, Wang C, Lee BS, Cohen GB, Jung JU.** 2000. Downregulation of major histocompatibility complex class I molecules by Kaposi's sarcoma-associated herpesvirus K3 and K5 proteins. J. Virol. **74:**5300–5309. http://dx.doi.org/10.1128/JVI.74.11.5300-5309.2000.
51. **Olp LN, Shea DM, White MK, Gondwe C, Kankasa C, Wood C.** 2013. Early childhood infection of Kaposi's sarcoma-associated herpesvirus in Zambian households: a molecular analysis. Int. J. Cancer **132:**1182–1190. http://dx.doi.org/10.1002/ijc.27729.
52. **Rimessi P, Bonaccorsi A, Stürzl M, Fabris M, Brocca-Cofano E, Caputo A, Melucci-Vigo G, Falchi M, Cafaro A, Cassai E, Ensoli B, Monini P.** 2001. Transcription pattern of human herpesvirus 8 open reading frame K3 in primary effusion lymphoma and Kaposi's sarcoma. J. Virol. **75:**7161–7174. http://dx.doi.org/10.1128/JVI.75.15.7161-7174.2001.
53. **Shamay M, Hand N, Lemas MV, Koon HB, Krown SE, Wrangle J, Desai P, Ramos JC, Ambinder RF.** 2012. CpG methylation as a tool to characterize cell-free Kaposi sarcoma herpesvirus DNA. J. Infect. Dis. **205:**1095–1099. http://dx.doi.org/10.1093/infdis/jis032.
54. **Minhas V, Crabtree KL, Chao A, M'Soka TJ, Kankasa C, Bulterys M, Mitchell CD, Wood C.** 2008. Early childhood infection by human herpesvirus 8 in Zambia and the role of human immunodeficiency virus type 1 coinfection in a highly endemic area. Am. J. Epidemiol. **168:**311–320. http://dx.doi.org/10.1093/aje/kwn125.
55. **Zhou FC, Zhang YJ, Deng JH, Wang XP, Pan HY, Hettler E, Gao SJ.** 2002. Efficient infection by a recombinant Kaposi's sarcoma-associated herpesvirus cloned in a bacterial artificial chromosome: application for genetic analysis. J. Virol. **76:**6185–6196. http://dx.doi.org/10.1128/JVI.76.12.6185-6196.2002.
56. **Lu J, Verma SC, Cai Q, Robertson ES.** 2011. The single RBP-Jkappa site within the LANA promoter is crucial for establishing KSHV latency during primary infection. J. Virol. **85:**6148–6161. http://dx.doi.org/10.1128/JVI.02608-10.
57. **Dollard SC, Butler LM, Jones AM, Mermin JH, Chidzonga M, Chipato T, Shiboski CH, Brander C, Mosam A, Kiepiela P, Hladik W, Martin JN.** 2010. Substantial regional differences in human herpesvirus 8 seroprevalence in sub-Saharan Africa: insights on the origin of the "KS Belt." Int. J. Cancer **127:**2395–2401. http://dx.doi.org/10.1002/ijc.25235.
58. **Jha HC, AJ MP, Saha A, Banerjee S, Lu J, Robertson ES.** 2014. Epstein-Barr virus essential antigen EBNA3C attenuates H2AX expression. J. Virol. **88:**3776–3788. http://dx.doi.org/10.1128/JVI.03568-13.
59. **Jha HC, Lu J, Saha A, Cai Q, Banerjee S, Prasad MA, Robertson ES.** 2013. EBNA3C-mediated regulation of aurora kinase B contributes to Epstein-Barr virus-induced B-cell proliferation through modulation of the activities of the retinoblastoma protein and apoptotic caspases. J. Virol. **87:**12121–12138. http://dx.doi.org/10.1128/JVI.02379-13.
60. **Mitchell N, Deangelis JT, Tollefsbol TO.** 2011. Methylated-CpG island recovery assay. Methods Mol. Biol. **791:**125–133. http://dx.doi.org/10.1007/978-1-61779-316-5_10.
61. **Rauch T, Pfeifer GP.** 2005. Methylated-CpG island recovery assay: a new technique for the rapid detection of methylated-CpG islands in cancer. Lab. Invest. **85:**1172–1180. http://dx.doi.org/10.1038/labinvest.3700311.